Liquid Crystals
Publication details, including instructions for authors and subscription information:
http://www.informaworld.com/smpp/title~content=t713926090

Influence of the position and number of fluorine atoms and of the chiral moiety on a newly synthesized series with anticlinic properties

C. Da Cruz; J. C. Rouillon; J. P. Marcerou; N. Isaert; H. T. Nguyen

Online publication date: 06 August 2010

To cite this Article Da Cruz, C. , Rouillon, J. C. , Marcerou, J. P. , Isaert, N. and Nguyen, H. T.(2001) 'Influence of the position and number of fluorine atoms and of the chiral moiety on a newly synthesized series with anticlinic properties', Liquid Crystals, 28: 8, 1185 — 1192
To link to this Article: DOI: 10.1080/02678290110048778
URL: http://dx.doi.org/10.1080/02678290110048778

LIQUID CRYSTALS, 2001, VOL. 28, NO. 8, 1185–1192

Influence of the position and number of fluorine atoms and of the chiral moiety on a newly synthesized series with anticlinic properties

C. DA CRUZ, J. C. ROUILLON, J. P. MARCEROU, N. ISAERT† and H. T. NGUYEN*

Centre de Recherche Paul Pascal, Université de Bordeaux I, Avenue A. Schweitzer, F-33600 Pessac, France

†Laboratoire de Dynamique et Structure de Matériaux Moléculaires, Université de Lille 1, UFR de Physique, F-59655 Villeneuve d'Ascq Cedex, France

(*Received 14 October 2000; in final form 13 January 2001; accepted 19 January 2001*)

A series of trifluoro-substituted benzoate derivatives: (*S*)-1-ethylheptyl 4-[4-(4-alkyloxy-3-fluorobenzoyloxy)-3-fluorobenzoyloxy]-2-fluorobenzoates is reported. The short chain members ($n = 8$ to $n = 11$) display a direct SmC^*_A–SmA transition, whereas for longer chains a SmC* phase appears, but no ferrielectric phases are present, and a direct SmC^*_A–SmC* transition is obtained. The mesomorphic properties were studied by optical microscopy and DSC, and by electro-optical, helical pitch and optical rotatory power measurements. The effect of the number and position of the fluoro substituents, and the influence of the chiral moiety on the mesomorphic behaviour are discussed.

1. Introduction

Since the discovery of 'antiferroelectricity' in liquid crystals by Chandani *et al.* [1] in 1989, SmC^*_A phases have been paid much attention, especially for their display applications. Up to now, most 'antiferroelectric' liquid crystals (AFLCs) have been designed following the model of the first compound to exhibit the SmC^*_A phase, MHPOBC the formula of which is represented below:

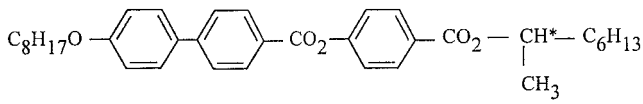

We have already reported the phase sequence Cr–SmC^*_A–SmC^*_{FI}–SmC*–SmC^*_α–SmA–I for the short chain members and CrK–SmC*–TGBA–I for the long chain homologues in the following series [2]:

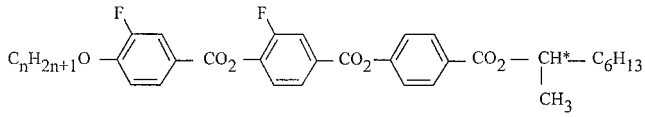

(*R*) Series I

The influence of the chiral moiety in several series on the existence of the SmC^*_A phase and on the SmA–SmC* or SmA–SmC^*_A transition was studied by different groups [3–6]. The direct SmA–SmC^*_A transition was observed when the ramification at the chiral centre is bigger than CH_3 (for example CF_3 or C_2H_5). We have explored several tolane series with different chiral chains. The series IIB was found to display an unusual mesomorphic behaviour. A direct first order transition between the SmC^*_A and SmA phases was obtained for the short members of this series. For the longer chain derivatives, an unusual 'isotropic' phase was detected for the first time in 'antiferroelectric' materials (L phase) [6].

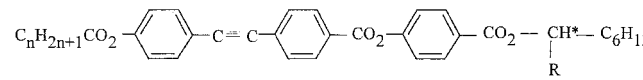

Series IIA where R = CH_3 (*R*)
IIB where R = C_2H_5 (*S*).

To emphasize the 'anticlinic' character in the tribenzoate series we modified the chemical structure by introducing the C_2H_5 group in the ramification instead of the CH_3 group on the chiral chain, and by substituting the hydrogen in position 2 of the first phenyl ring near the chiral centre by a fluorine.

In this paper, we report the synthesis and characterization of the following series:

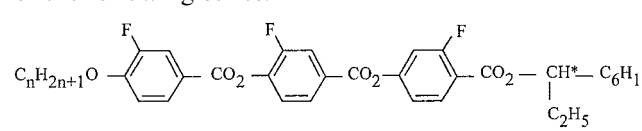

(*S*) series IIIB

*Author for correspondence; e-mail: tinh@crpp.u-bordeaux.fr

Liquid Crystals ISSN 0267-8292 print/ISSN 1366-5855 online © 2001 Taylor & Francis Ltd
http://www.tandf.co.uk/journals
DOI: 10.1080/02678290110048778

2. Synthesis and mesomorphic properties

The materials studied in this paper were synthesized following the scheme. The 4-alkyloxy-3-fluorobenzoic acids and 4-benzyloxy-3-fluorobenzoic acid were prepared by well known methods [2, 7].

All the compounds are mesomorphic. The phase behaviour and transition temperatures of the members of this chiral series are summarized in the table. They were determined both by thermal microscopy (Mettler FP5) and differential scanning calorimetry (Perkin-Elmer DSC 7). Heating and cooling rates were 2°C min^{-1}. The compounds display SmA and SmC^*_A phases over the entire series and a SmC* phase appears for the compounds with $n = 12$ and $n = 14$.

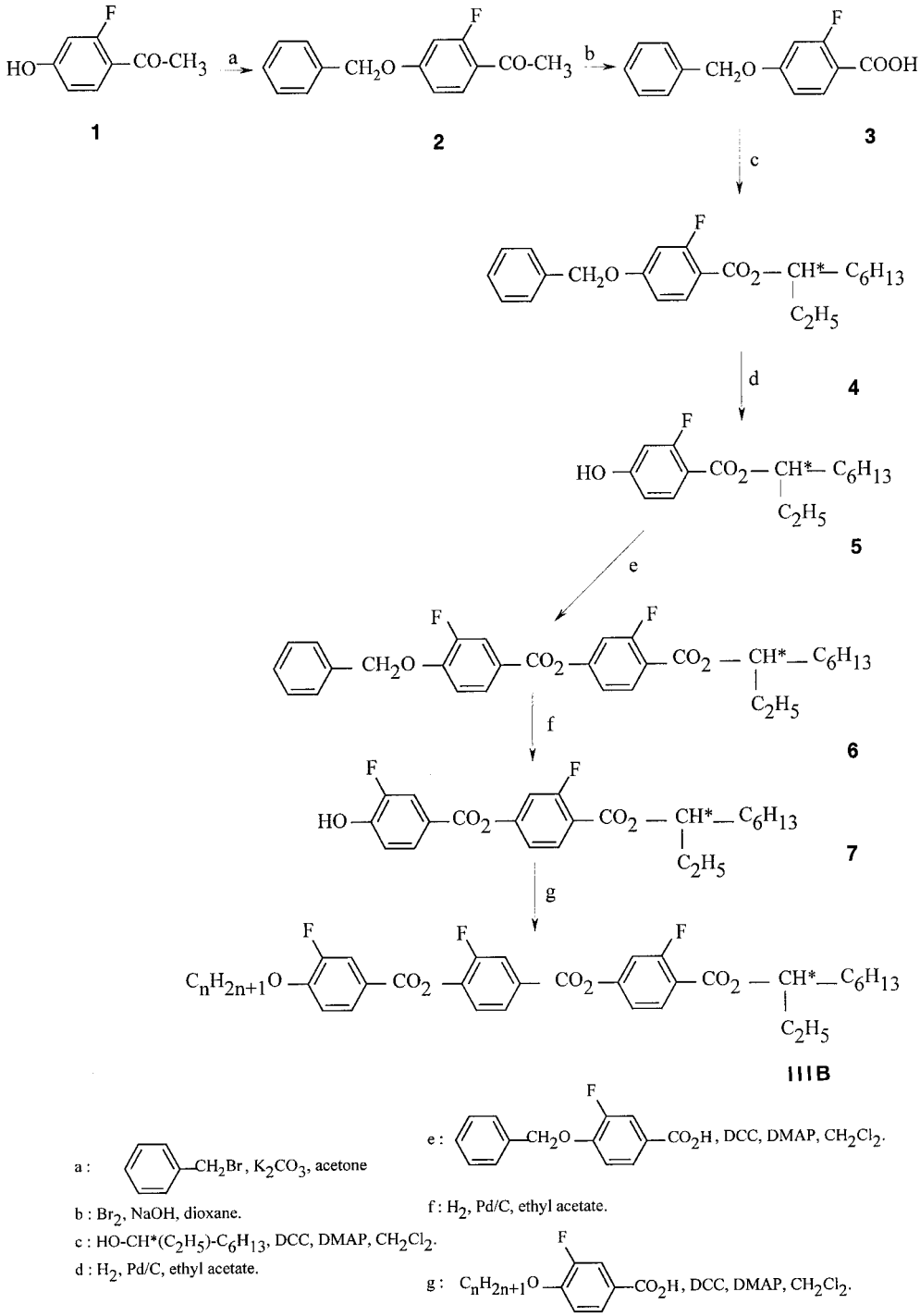

Scheme. Synthetic route to series IIIB.

Table. Transition temperatures (°C) and enthalpies (in italics, kJ mol^{-1}) for the series IIIB: DSC scanning rate 2°C min^{-1}.

n	Cr		SmC^*_A		SmC*		SmA		I
8	•	49.1 *18.657*	•	74.7 *0.406*	—		•	90.4 *3.897*	•
9	•	62.4 *15.09*	•	73.6 *0.554*	—		•	87 *3.722*	•
10	•	71.3 *20.28*	•	76.7 *0.705*	—		•	85.6 *3.51*	•
11	•	63.2 *28.008*	•	75.5 *0.871*	•[c]		•	83.0 *3.282*	•
12[a]	•	40.9 *22.485*	•	75.5	• *0.835*[d]	76.8	•	83.3 *3.349*	•
14[a]	•	54.5 *31.608*	•	65.1[b] *0.018*	•	76.9 *0.325*	•	85.5 *3.42*	•

[a] DSC scanning rate 2°C min^{-1}.
[b] Transition SmC^*_A–SmC^*_{FI}–SmC*.
[c] The SmC* phase exists over a very short range.
[d] Enthalpies summed for the transitions SmC^*_A–SmC* and SmC*–SmA.

For compounds $n = 8$, 9 and 10, a direct SmC^*_A–SmA transition is observed without the presence of the SmC* phase. The existence of the 'antiferroelectric' phase is proved by the electro-optical studies on compound $n = 10$, made because we could not distinguish by microscopic observations if the phase was a SmC^*_A or a SmC* phase. Indeed, electro-optical measurements show a high threshold field, over 2.6 V μm, only one degree below the SmC^*_A–SmA transition, a threshold that increases with decreasing temperature.

For the compound $n = 11$, DSC measurements show various overlapping peaks indicating the presence of various phase transitions in a range of 0.5°C which forbids us from studying them independently at the SmC^*_A–SmA transition. The SmC* phase certainly begins to appear but with a very short range.

For the compound $n = 12$ we obtain a direct transition from SmC^*_A to SmC* without any ferrielectric phase that could be observed by microscopy or DSC. If any ferrielectric phase exists the temperature range is so very small that we could not study it. This direct transition was further studied and explained by helical pitch and electro-optical measurements, as described later.

Summarising the situation for the compound $n = 12$, on cooling from the isotropic liquid, we can observe, in sequence, the SmA phase with very coloured focal-conic textures and homeotropic domains at $T = 77$°C, the SmC* phase with striated fan-shaped pseudo-homeotro pic textures at $T = 74$°C and finally the SmC^*_A phase at $T = 70$°C, similar in appearance to the SmC* phase, but distinguishable by electro-optical studies because of its threshold field. The temperature range of existence for the SmC* phase is very small, only 1.3°C.

Finally, the compound $n = 14$ gives a SmC* phase over 11.8°C, much larger than with that for the compound $n = 12$. By increasing the chain carbon number, the SmC* phase is stabilized whereas the SmC^*_A phase is destabilized.

3. Helical pitch measurements

We performed pitch measurements on the SmC^*_A and SmC* phases of the $n = 12$ derivative using prismatic samples oriented in the Grandjean–Cano geometry and free surface homeotropic drops [8].

The helical pitch is quasi-constant: 0.39 μm in the SmC^*_A phase, a value in keeping with the orange coloured selective reflection; 0.49 μm in the SmC* phase (dark red selective reflection); a perceptible decrease (0.47 μm) precedes the transition to the SmA phase.

The sign of the rotatory power, right in the SmC^*_A phase and left in the SmC* phase (for $\lambda = 0.546$ μm), shows that the helix handedness changes between the two phases: left handed in the SmC* phase, the helix becomes right handed in the SmC^*_A phase. These conclusions are also confirmed by the analysis of the circularly polarized reflected light.

These optical studies confirm that, besides the phase sequence with a short SmC* phase between SmC^*_A and SmA, there is no SmC^*_{FI} phase; also, the free surface homeotropic drop observations excluded any SmC^*_α phase.

We also performed optical rotatory power (ORP) measurements at a wavelength λ of 632.8 nm that confirm the Grandjean–Cano results (figure 1). We see in the upper range of the SmC* phase that the measured angle is negative, showing that the helix is low pitch and left handed ($\lambda/n \sim 0.42\,\mu\text{m} > -p > 0$, where p is the helix pitch and n the mean in-plane index of refraction). Then when cooling, the pitch slightly increases, crossing the selective reflection regime at about 78.1°C, leading to a divergence of the ORP; one then enters a large

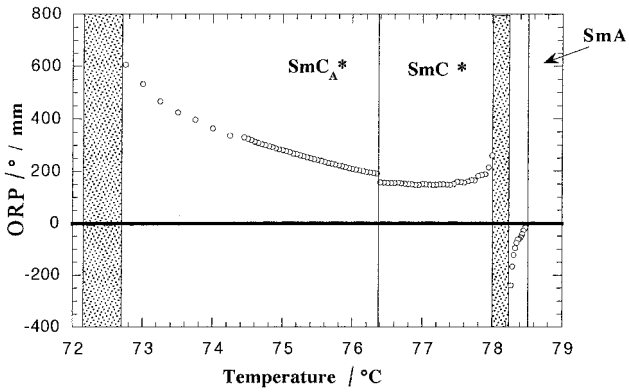

Figure 1. Optical rotatory power at 632.8 nm for a 100 μm thick homeotropic sample of the $n = 12$ compound.

pitch domain ($-p > \lambda/n \sim 0.42\,\mu m > 0$) with positive ORP. Finally in the SmC$_A^*$ phase, the ORP stays positive as we enter a low pitch right handed domain ($\lambda/n \sim 0.42\,\mu m > +p > 0$), with a slightly increasing pitch on further cooling and approaching a new selective reflection at ~ 72.7°C.

4. Electro-optical studies

Electro-optical properties were studied using the SSFLC configuration to evaluate polarization, response time, and tilt angle in a single set-up. Commercial cells (EHC from Japan) coated with indium tin oxide (ITO) and rubbed polyimide were used. The thickness of the cells was around 15 μm; the active area was 0.25 cm^2. Slow cooling from the isotropic liquid to SmA phase transition (0.1°C min^{-1}) leads to planar alignment. The compound with $n = 12$ was studied and the measurements were made upon cooling to facilitate the alignment.

We note a gap of one to two degrees observed between the electro-optical and DSC measurements for the transition temperatures due to the high rate of heating (DSC) and miscalibration of the hot stage.

The polarization was calculated by integration of the switching current under a rectangular a.c. field at 41 Hz. The field value was 5.3 V μm^{-1}, sufficient to unwind the helical structure and accomplish the phase transition from the SmC$_A^*$ and SmC* phases to the unwound SmC* phase. As pictured in figure 2, the polarization versus temperature plot shows no anomalies at the phase transition temperatures. The values of the saturated polarizations are not very high, being similar to those for many three-ring compounds. The plateau value is around 82 nC cm^{-2} at $T = 70$°C and the polarization diminishes 36 nC cm^{-2} at the phase transition SmC*–SmA (figure 2).

We used a square wave voltage of 5.3 V μm^{-1} for the response time measurement. The electric response time is the time required for the majority of the molecules to switch under the applied field. The electric response time decreases with increasing temperature and changes from 78 μs at $T = 70$°C to 37 μs at $T = 78.5$°C (figure 3).

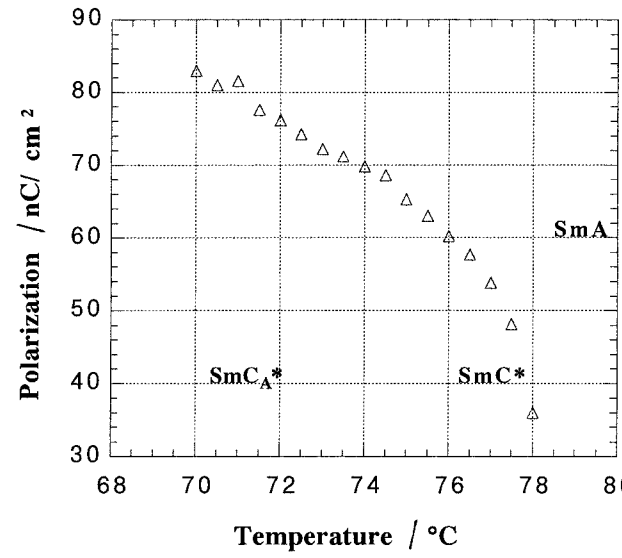

Figure 2. Temperature dependence of the polarization at saturation ($\mathbf{E} = 5.3$ V μm^{-1}, $v = 41$ Hz) for $n = 12$.

The apparent tilt angle θ of the molecules from the smectic layer normal was calculated from the difference between the extinction positions of the sample between crossed polarizers under a rectangular a.c. field (5.3 V μm^{-1}) at very low frequency (0.1 Hz). The accuracy of the measurement was estimated at ± 3° (figure 4). The tilt angle seems to have a plateau value around 32° and slowly diminishes.

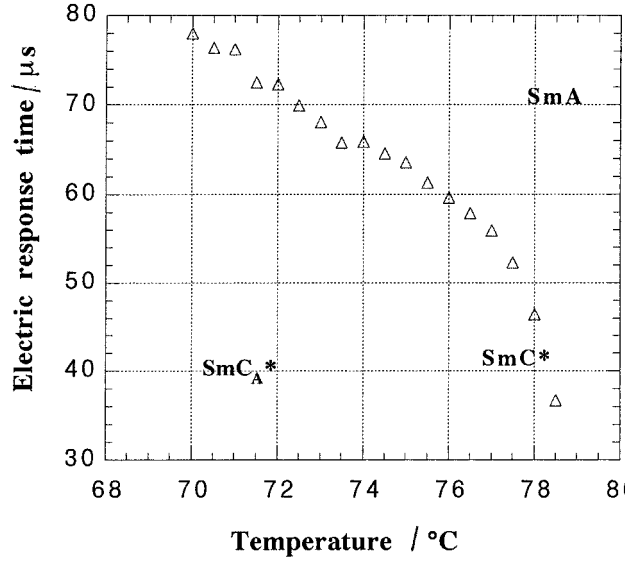

Figure 3. Temperature dependence of the electric response time ($\mathbf{E} = 5.3$ V μm^{-1}, $v = 41$ Hz) for $n = 12$.

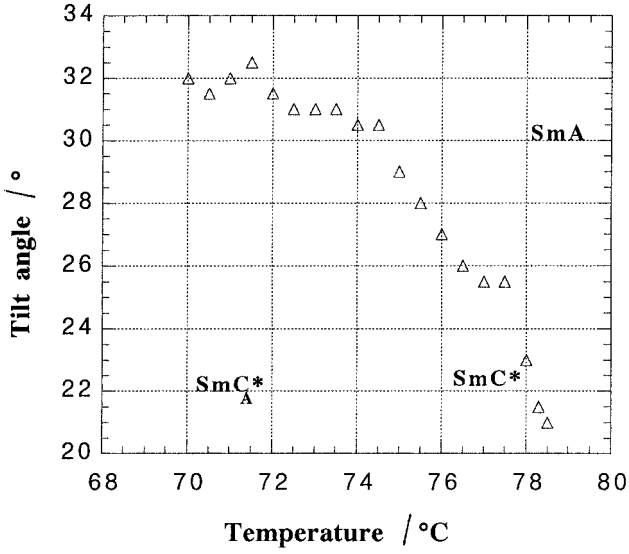

Figure 4. Temperature dependence of the apparent tilt angle ($\mathbf{E} = 5.3$ V μm^{-1}, $\nu = 0.1$ Hz) for $n = 12$.

Note that working with ordinary triangular electric fields of 5 V μm^{-1} at 41 Hz, in the vicinity of the SmA–SmC* phase transition of the C12 compound, one recovers a current reversal form with two peaks per half-period, which is currently assumed to be the signature of the so-called 'antiferroelectric' phase (figure 5). On the contrary, in the temperature range of the anticlinic phase, under the same conditions, one observes only one peak per half-period which would immediately lead to the conclusion that the phase is not 'antiferroelectric'. This is an illustration of the misleading character of phase

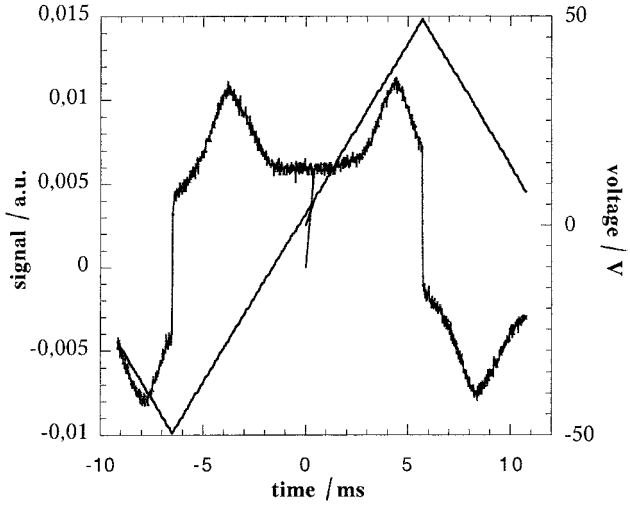

Figure 5. Switching current in the vicinity of the SmA–SmC* phase transition at $\mathbf{E} = 3.3$ V μm^{-1}, $\nu = 41$ Hz, $T = 78.3$°C under a triangular electric field, for the $n = 12$ compound.

determination derived from peak counting arguments, which may indeed lead to sterile polemics as in the case of the first reported 'banana-like' compound (PIMB) which possesses a mesophase, ferroelectric or antiferroelectric, according to different groups [9]. In our case, the unusual results obtained in the series under study may be explained in the following way.

Firstly, in the high temperature range of the C12 compound, the SmA to SmC* phase transition is discontinuous and first order. Moreover under an electric field, as for the old valine or isoleucine biphenyl series [10, 11], this transition transforms a low angle SmC* to a large angle SmC* mapped in the T–$\mathbf{E}$ plane by a first order line ending at a critical point [12]. The critical field $\mathbf{E}_c$ is probably in the range of a few V μm^{-1}, while the critical temperature, T_c is a few tenths of a degree above the zero field transition temperature, T_{ac} (~ 78.3°C for T_c and 78°C for T_{ac}). If the frequency of the triangular voltage (41 Hz) is not too large, in order to allow enough time for the phase transitions to occur, a part of the system at least is continuously switching from low angle paraelectric SmC* to large angle ferroelectric phase, giving birth to a current peak at each transition. As there are two phase transitions per half-period, one recovers the 'classical antiferroelectric' current curve (figure 5). Then if the temperature is slightly decreased, one crosses twice the first order line per half-period and a part of the sample stays in the ferroelectric large angle SmC* phase coexisting with another switching part leading to the above 'antiferroelectric' doublet. Finally at lower temperatures, the ferroelectric SmC* phase dominates and one recovers the expected unique peak.

Secondly, in the anticlinic phase, the artefact is due to the rather slow kinetics of the field-induced phase transition between the paraelectric anticlinic SmC^*_A and the ferroelectric SmC* phases. At a working frequency of 41 Hz, with a peak voltage much higher than the threshold voltage, all the sample stays in the metastable ferroelectric phase and the polarization switches from $-$P to $+$P leading to a single peak per half-period. In order to recover the much to be expected double peak, one has to lower the working frequency and use a truncated triangular voltage shape to allow enough time for the ferroelectric–paraelectric phase transition to occur. This has been sketched in figure 6 with a 0.3 Hz frequency.

5. Discussion and conclusion

We have already reported the 'anticlinic' character of the series I [2]. To obtain more information, we introduced a fluorine in position 2 of the phenyl ring near the chiral group (series IIIA), and modified the ramification at the chiral centre (series III A, B, C). First, we compare

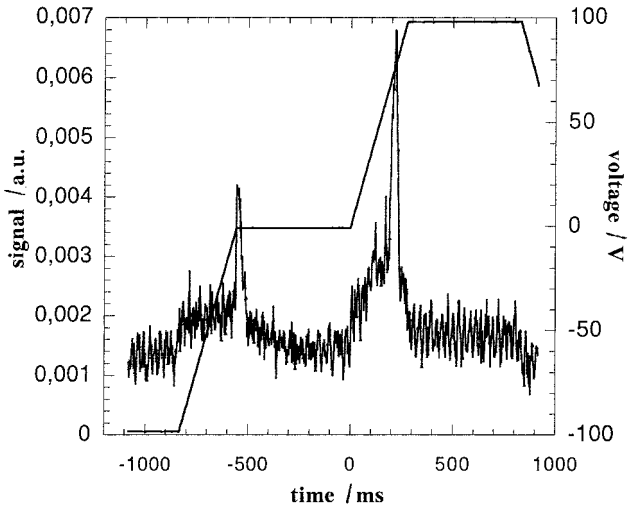

Figure 6. Switching current in the temperature range of the anticlinic phase at $\mathbf{E} = 6.7\ \mathrm{V\ \mu m^{-1}}$, $v = 0.3$ Hz, $T = 74°C$ under a truncated triangular field for the $n = 10$ compound.

the compounds $n = 10$ of series I and IIIA which differ only in the presence or absence of the fluorine near the chiral chain.

Cr 57.7 SmC_A^* 80.6 SmC_{FI}^* 83.5 SmC* 93.9 SmC_α 94.5 SmA 103.7 I (°C) series I

Cr 74.1 SmC_A^* 95.3 SmC_{FI}^* 95.6 SmC* 101.5 SmA 110 I (°C) series IIIA.

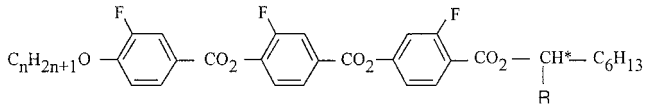

Series IIIA, R = CH_3; IIIB, R = C_2H_5; IIIC, R = C_3H_7.

In fact, the ferrielectric phase range is reduced and exists only over 0.3°C in the $n = 10$ compound of series IIIA, and the temperature range for the SmC* phase is 5.9°C. Therefore we can see that whereas the sum of the ferrielectric and ferroelectric phase ranges of the $n = 10$ compound (series IIIA) with a fluorine in position 2 is smaller than that of the $n = 10$ compound of series I, the SmC_A^* temperature range is increased. We can say positively that the presence of this fluorine in position 2 favours the anticlinic phase. However the presence of this fluorine is not enough to produce a direct SmC_A^*–SmA transition. To obtain this, the size of the side chiral group seems to be an essential parameter. Besides, when a substituent is introduced into a system the clarification temperature of the compound generally decreases. However, in this case the fluorine increases it, giving us the hope of obtaining some interesting compounds with a bigger R group. We therefore prepared the compounds of series IIIB and IIIC with $n = 10$.

Cr 74.1 SmC_A^* 95.3 SmC_{FI}^* 95.6 SmC* 101.5 SmA 110 I (°C) series IIIA, R = CH_3

Cr 71.3 SmC_A^* 76.7 SmA 85.6 I (°C) series IIIB, R = C_2H_5

Cr 65.5 SmC_A^* (56.2) SmA 68.6 I (°C) series IIIC, R = C_3H_7.

Now we compare the compounds $n = 10$ with a CH_3 group and a C_2H_5 group. We can see that the replacement of the methyl group attached to the chiral carbon by an ethyl group appears to stabilize the SmC_A^* phase strongly with respect to other possible helical smectic phases for the compounds. All helical smectic phases usually observed between SmC_A^* and SmA phases, i.e. ferrielectric phases SmC* and SmC_α^*, in fact disappear and a first order SmC_A^*–SmA transition is observed instead. Similar trends have been reported for AFLC compounds bearing different chiral chains, notably when the side group on the asymmetric carbon was a CF_3 or C_2F_5 group [13]. Nishiyama *et al.* [5] studied a series with a biphenyl ring system and obtained a direct SmC_A–SmA transition (but the SmC_A phase was monotropic) with a propyl group, but not with ethyl. Two parameters have to be taken into account to induce this direct transition: first, the side chiral group has to be big enough and second, the rigid core structure itself has to favour anticlinic phases.

With a bigger group R (C_3H_7) over all the series IIIC a direct SmC_A^*–SmA transition is observed; the SmC_A^* phase is now monotropic for $n = 10$, but then becomes enantiotropic until $n = 18$. However, for the entire series, the temperature interval between the SmC_A^* and the SmA phases is constant around 10°C. Hope for the existence of a TGB phase is thus totally excluded.

However, the effect of increasing the alkyl chain length was disappointing. Indeed, because series I gave TGBA phases for the longest chain compounds, with the increased anticlinic character of series I through introducing the fluorine and increasing the tendency for direct SmC_A^*–SmA transitions, we hoped to obtain the TGB phases with anticlinic properties owing to the enhanced rotatory power (due to the presence of the fluorines near the alkyl chain) that could twist the SmA blocks. The presence of the SmC* phase however rules out the formation of such a $TGBC_A^*$ phase. Perhaps the structure of our series is not quite appropriate in favouring anticlinic phases sufficiently to exclude totally the SmC* phase even for the longest chain members.

6. Experimental

The NMR spectra were recorded on a Bruker HW 300 MHz spectrometer. The infrared spectra were recorded on a Perkin-Elmer 783 spectrophotometer. The following examples are typical of the synthetic methods used to obtain the compounds given in the table.

6.1. *4-Benzyloxy-2-fluoroacetophenone (**2**)*

Benzyl bromide (3.8 ml, 32.0 mmol) in acetone (20 ml) was added dropwise to a mixture of 2-fluoro-4-hydroxy-acetophenone (5.0 g, 32.0 mmol), potassium carbonate (11 g, 80 mmol) and acetone (100 ml). The resulting mixture was heated at reflux and stirred for 16 h. The cooled reaction mixture was then filtered to remove excess of potassium carbonate and precipitated potassium bromide. The filtrate was evaporated, treated with diethyl ether (200 ml), washed with water (2×100 ml) and the organic layer dried over Na_2SO_4 and filtered. The solvent was evaporated under reduced pressure to give a solid which was purified by column chromatography (silicagel, 9:1 heptane–ethyl acetate) to give a white powder which was recrystallized from absolute ethanol; yield = 4.8 g (62%).

6.2. *4-Benzyloxy-2-fluorobenzoic acid (**3**)*

Bromine (29.5 g, 0.18 mol) was added dropwise to a cooled (< 0°C), stirred solution of NaOH (30 g, 0.74 mol) in water (150 ml). This solution was added dropwise to a cooled solution of the acetophenone **2** previously synthesized (3 g, 12.3 mmol) in dioxan. The reaction mixture was stirred at room temperature for 1 h and then maintained at 30–35°C for 2 h. To the cooled solution, a 40% sodium bisphite solution (20 ml) was added; the resulting solution was hydrolysed with hydrochloric acid (100 ml) and crushed ice. The precipitated acid was filtered off and recrystallized from absolute ethanol; yield = 2.9 g (97%). ^{1}H NMR ($CDCl_3$, ppm): 1.25 (s, 1H, −COOH), 5.1 (s, 2H, CH_2−O), 6.8 (m, 2H arom. *ortho* and *para* to F), 7.4 (m, 5H arom.), 8 (t, 1H arom. *meta* to F). IR (KBr) (cm^{-1}): 2950 (OH), 1702, 1676 (C=O), 1619, 1502, 1446 (C=C phenyl rings).

6.3. *(S)-1-Ethylheptyl 4-benzyloxy-2-fluorobenzoate (**4**)*

To a solution of (*S*)-3-nonanol (1.04 g, 7.2 mmol) in CH_2Cl_2 (70 ml) was added DCC (1.7 g, 7.2 mmol), DMAP (0.07 g) and 4-benzyloxy-2-fluorobenzoic acid (1.8 g, 7.2 mmol). The resulting solution was stirred at room temperature overnight, filtered, and the solvent evaporated. The residue was chromatographed on silica gel with CH_2Cl_2 as eluent. The product was used without purification; yield = 1.6 g (60%). ^{1}H NMR ($CDCl_3$, ppm): 0.9 (m, 6H, CH_3 of C_6H_{13}, CH_3 of C_2H_5), 1.3 (m, 8H, $4CH_2$ of C_6H_{13}), 1.6 (m, 4H, $2CH_2$ on the α position of the chiral carbon), 5.1 (m, 1H, O−<u>CH</u>−CH_2−), 6.65 (m, 2H arom. *ortho* and *para* to F), 7.4 (m, 5H arom.), 7.8 (t, 1H arom. *meta* to F).

6.4. *(S)-1-Ethylheptyl 4-hydroxy-2-fluorobenzoate (**5**)*

To a solution of compound **4** (2.14 g, 5.75 mmol) in 200 ml of ethyl acetate was added 0.22 g of Pd/C. Hydrogen was applied under a slight pressure. When the reaction was complete the catalyst was filtered off and the solvent evaporated. As the reaction is quantitative, the liquid phenol was used in the next step without further purification; yield = 1.3 g (80%). ^{1}H NMR ($CDCl_3$, ppm): 0.9 (m, 6H, CH_3 of C_6H_{13}, CH_3 of C_2H_5), 1.3 (m, 8H, $4CH_2$ of C_6H_{13}), 1.6 (m, 4H, $2CH_2$ on the α position of the chiral carbon), 5.1 (m, 1H, O−<u>CH</u>−CH_2−), 6.3 (s, 1H, O−H), 6.65 (m, 2H arom. *ortho* and *para* to F), 7.8 (t, 1H arom. *meta* to F).

6.5. *(S)-1-Ethylheptyl 4-(4-benzyloxy-3-fluorobenzoyloxy)-2-fluorobenzoate (**6**)*

To a solution of phenol **5** (1.3 g, 4.6 mmol) in CH_2Cl_2 (50 ml) was added DCC (1.2 g, 4.6 mmol), DMAP (0.05 g) and 4-benzyloxy-3-fluorobenzoic acid (1.13 g, 4.6 mmol). The resulting mixture was stirred at room temperature overnight. The mixture was then filtered and the solvent evaporated. The residue was chromatographed on silica gel using CH_2Cl_2 as eluent. The product (white powder) was used without further purification; yield = 1.2 g (51%). ^{1}H NMR ($CDCl_3$, ppm): 0.9 (m, 6H, CH_3 of C_6H_{13} and CH_3 of C_2H_5), 1.3 (m, 8H, $4CH_2$ of C_6H_{13}), 1.7 (m, 4H, $2CH_2$ on the α position of the chiral carbon), 5.1 (m, 1H, O−<u>CH</u>−CH_2−), 5.2 (s, 2H, −CH_2−O−), 7.1 (m, 3H arom., 2H *ortho* and *para* to F of the first ring and 1H *meta* to F of the second ring), 7.4 (m, 5H arom.), 7.9 (m, 3H arom., 1H *meta* to F of the first ring, 2H *ortho* and *para* to F of the second ring). IR (KBr) (cm^{-1}): 2958, 2927, 2858 (C−H aliphatic), 1733, 1718 (C=O), 1616, 1521, 1434 (C=C phenyl rings).

6.6. *(S)-1-Ethylheptyl 4-(4-hydroxy-3-fluorobenzoyloxy)-2-fluorobenzoate (**7**)*

To a solution of compound **6** (1.2 g, 2.35 mmol) dissolved in 150 ml of ethyl acetate was added 0.15 g of Pd/C. The mixture was stirred under a slight pressure of hydrogen. When the reaction was complete, the catalyst was filtered off and the solvent evaporated. The liquid phenol was used without purification; yield = 0.9 g (91.2%). ^{1}H NMR ($CDCl_3$, ppm): 0.9 (m, 6H, CH_3 of C_6H_{13} and CH_3 of C_2H_5), 1.3 (m, 8H, $4CH_2$ of C_6H_{13}), 1.7 (m, 4H, $2CH_2$ on the α position of the chiral carbon), 5.1 (m, 1H, O−<u>CH</u>−CH_2−), 6 (large s, 1H, O−H), 7.15 (m, 3H arom., 2H *ortho* and *para* to F of the first ring and 1H *meta* to F of the second ring), 7.95 (m, 3H arom., 1H *meta* to F of the first ring, 2H *ortho* and *para* to F of the second ring). IR (KBr) (cm^{-1}): 2958, 2927, 2858 (C−H aliphatic), 1733, 1718 (C=O), 1616, 1521, 1434 (C=C phenyl rings).

6.7. *(S)-1-Ethylheptyl 4-[4-(4-dodecyloxy-3-fluorobenzoyloxy)-3-fluorobenzoyloxy]-2-fluorobenzoate (**8**)*

4-Dodecyloxy-3-fluorobenzoïc acid (0.16 g, 0.5 mmol) was added to a solution of phenol **7** (0.21 g, 0.5 mmol),

DCC (0.12 g, 0.5 mmol) and DMAP (0.005 g) dissolved in CH_2Cl_2 (5 ml). The mixture was stirred overnight at room temperature; it was filtered and the solvent evaporated. The residue was purified by chromatography on silica gel using toluene as eluent. The product was recrystallized from absolute ethanol; yield = 0.2 g (55%). ^{1}H NMR ($CDCl_3$, ppm): 0.8–1 (m, 9H, CH_3 of C_6H_{13}, CH_3 of $C_{12}H_{25}$, CH_3 of C_2H_5), 1.2–1.5 (m, 26H, $9CH_2$ of $C_{12}H_{25}$, $4CH_2$ of C_6H_{13}), 1.6–1.8 (m, 6H, $2CH_{2\beta}$ and CH_2 of C_2H_5), 4.1 (t, 2H, $-\underline{CH_2}-O$), 5.1 (m, 1H, $O-\underline{CH}-CH_2-$), 7.1 (m, 3H arom., 2H *ortho* and *para* to F of the first ring and 1H *meta* to F of the second ring), 7.45 (t, 1H arom. *meta* to F of the third ring), 8 (m, 5H arom., 1H *meta* to F of the first ring, 2H *ortho* and *para* to F of the second ring, 2H *ortho* and *para* to F of the third ring). IR (KBr) (cm^{-1}): 2953, 2925, 2854 (C–H aliphatic), 1752, 1742, 1705 (C=O), 1616, 1519, 1438 (C=C phenyl rings).

One of us, C. Da Cruz, wishes to thank Praxis XXI for financial support.

References

[1] Chandani, A. D. L., Ouchi, Y., Takezoe, H., Fukuda, A., Furukawa, K., and Kichi, A., 1989, *Jpn. J. appl. Phys.*, **28,** 1261.

[2] Da Cruz, C., Rouillon, J. C., Marcerou, J. P., Isaert, N., and Nguyen, H. T, 2001, *Liq. Cryst.*, **28,** 125.

[3] Suzuki, Y., Kitazume, T., Kakimoto, M., Ouchi, Y., Takezoe, H., and Fukuda, A., 1989, *Liq. Cryst.*, **6,** 167.

[4] Ouchi, Y., Kitamura, M., and Nishiyama, I., 1995, *J. mater. Chem.*, **5,** 2297.

[5] Nishiyama, I., and Goodby, J. W., 1993, *J. mater. Chem.*, **3,** 149.

[6] Faye, V., Rouillon, J. C., Nguyen, H. T., Dètrè, L., Laux, V., and Isaert, N., 1998, *Liq. Cryst.*, **24,** 747.

[7] Nabor, M. F., Nguyen, H. T., Destrade, C., Marcerou, J. P., and Twieg, R. J., 1991, *Liq. Cryst.*, **10,** 785.

[8] Laux, V., Isaert, N., Joly, G., and Nguyen, H. T., 1999, *Liq. Cryst.*, **26,** 361.

[9] (*a*) Niori, T., Sekine, T., Watanabe, J., Furukawa, T., and Takezoe, H., 1996, *J. mater. Chem.*, **6,** 1231; (*b*) Diele, S., Grande, S., Kruth, H., Lischka, Ch., Pelzl, G., Weissflog, W., and Wirth, I., 1998, *Ferroelectrics*, **212,** 169.

[10] Bahr, Ch., Heppke, G., and Sabaschus, B., 1988, *Ferroelectrics*, **84,** 103.

[11] Dupont, L., Galvan, J. M., Marcerou, J. P., and Prost, J., 1988, *Ferroelectrics*, **84,** 317.

[12] Prost, J., and Dèfontaines, A. D., 1993, *Phys. Rev. E*, **47,** 1184.

[13] Suzuki, Y., Nonaka, O., Koide, Y., Okabe, N., Hagiwara, T., Kawamura, I., Yamamoto, N., Yamada, Y., and Kitzume, T., 1993, *Ferroelectrics*, **147,** 109.